

**The Clusters AgeS Experiment (CASE):
V209 ω Cen – An Eclipsing Post-Common Envelope Binary
in the Globular Cluster ω Cen¹**

J. Kaluzny², S. M. Rucinski³, I. B. Thompson⁴, W. Pych² and W. Krzeminski⁵

ABSTRACT

We use photometric and spectroscopic observations of the detached eclipsing binary V209 ω Cen to derive the masses, radii, and luminosities of the component stars. The system exhibits total eclipses and, based on the measured systemic velocity and the derived distance, is a member of the globular cluster ω Cen. We obtain $0.945 \pm 0.043 M_{\odot}$, $0.983 \pm 0.015 R_{\odot}$ and $6.68 \pm 0.88 L_{\odot}$ for the cooler, but larger and more luminous primary component. The secondary component has $0.144 \pm 0.008 M_{\odot}$, $0.425 \pm 0.008 R_{\odot}$ and $2.26 \pm 0.28 L_{\odot}$. The effective temperatures are estimated at 9370 K for the primary and at 10866 K for the secondary. On the color-magnitude diagram of the cluster, the primary component occupies a position between the tip of the blue straggler region and the extended horizontal branch while the secondary component is located close to the red border of the area occupied by hot subdwarfs. However, its radius is too large and its effective temperature is too low for it to be an sdB star. We propose a scenario leading to the formation of a system with such unusual properties with the primary component “re-born” from a former white dwarf which accreted a new envelope through mass transfer from its companion. The secondary star has lost most of its envelope while starting its ascent onto the sub-giant branch. It failed to ignite helium in its core and is currently powered by a hydrogen burning shell.

Subject headings: binaries: close – binaries: spectroscopic – stars: individual (V209 ω Cen) – globular clusters: individual (ω Cen)

²Copernicus Astronomical Center, Bartycka 18, 00-716 Warsaw, Poland; (jka,pych)@camk.edu.pl

³David Dunlap Observatory, Department of Astronomy and Astrophysics, University of Toronto, P.O. Box 360, Richmond Hill, ON L4C 4Y6, Canada; rucinski@astro.utoronto.ca

⁴Carnegie Observatories, 813 Santa Barbara St., Pasadena, CA 91101-1292; ian@ociw.edu

⁵Las Campanas Observatory, Casilla 601, La Serena, Chile; wojtek@lco.cl

¹This paper utilizes data obtained with the 6.5-meter Magellan Telescopes located at Las Campanas Observatory, Chile.

1. INTRODUCTION

The study of globular cluster sdB stars has progressed significantly in the last few years from both a observational and theoretical perspective (see the extensive Introduction in Moni-Bidin et al. (2006a)). A particularly important question whether short-period, close binaries are very common (Maxted et al. 2001) or very rare (Moni-Bidin et al. 2006a) among the sdB stars urgently requires resolution; note that the first paper deals with the field objects while the latter is related to the population of the globular cluster NGC 6752. It is not excluded that environmental effects are responsible for the observed difference. Based on the results from the SPY radial velocity survey, Napiwotzki et al. (2004) obtained 39% for the relative frequency of spectroscopic sdB binaries among field stars.

As part of the Las Campanas CASE project, a study of eclipsing binaries in globular clusters (Kaluzny et al. 2005), we present in this paper photometric and spectroscopic observations of the eclipsing sdB binary V209 in the globular cluster ω Cen. The binary V209 ω Cen in the catalogue of Clement et al. (2001) (also known as OGLE-GC14; from now on called V209) was discovered by Kaluzny et al. (1996) during a survey for variable stars in the field of the globular cluster ω Cen. They presented a V -band light curve of the variable and found an orbital period of $P = 0.8344$ d. Further BV photometry of V209 together with a finding chart were published by Kaluzny et al. (2004). On the $V/(B - V)$ color-magnitude diagram of the cluster the variable occupies a position at the top/blue edge of the blue straggler sequence. In this paper we report photometric and spectroscopic observations aimed at a determination of the absolute parameters of V209.

2. PHOTOMETRIC OBSERVATIONS AND REDUCTIONS

The photometric data were obtained with the 2.5-m du Pont telescope at Las Campanas Observatory. A field of 8.65×8.65 arcmin was observed with the TEK#5 CCD camera at a scale of $0.259''/\text{pixel}$. A large fraction of the frames were collected in a subraster mode with the actual field of view reduced to 8.65×4.32 arcmin. Observations were collected during the 1997, 1998 and 2003 observing seasons. In 1997 and 1998 we used BV filters while in 2003 we used mostly VI filters with some additional UB observations taken on a single night when several Landolt (1992) photometric standard fields were also observed. A summary of the photometric data is given in Table 1. The raw data were pre-processed with the IRAF-

CCDPROC package². Time series photometric data were extracted using the ISIS-2.1 image subtraction package (Alard & Lupton 1998; Alard 2000). Our procedure closely followed that described in detail by Mochejska et al. (2002). Zero points for the ISIS instrumental magnitude differential light curves were determined from the template images using the DAOPHOT/ALLSTAR package (Stetson 1987). Aperture corrections were measured with the DAOGROW program (Stetson 1990). When determining the photometric zero points we took into account the flux from a close visual companion to V209. This companion is located about 0.1 arcsec East and 0.5 arcsec South of the variable and has $V = 20.77 \pm 0.10$, $B - V = 0.53 \pm 0.27$, and $V - I = 0.66 \pm 0.16$. The companion was unambiguously detected on the stacked template images with seeing of 0.67–0.70 arcsec. To minimize the effects of a variable point spread function we used 600×600 pixel sub-images in the ISIS analysis. In order to reduce the effects of crowding, the variable was located in the south-west corner of the analyzed field; at the position of V209 in the cluster there is still a noticeable gradient of the stellar surface density. The lower crowding helped in the measurement of accurate aperture corrections.

2.1. Photometric Calibration and the Light Curve

We observed the field of V209 along with several Landolt (1992) fields on the photometric night 2003 May 4/5. Specifically, 9 *UBVI* observations of 7 standard fields were collected, with two fields observed twice. In total, we obtained 39 *UBVI* measurements for 31 standard stars. The standards were observed with a range of air-mass $1.06 < X < 1.80$ while the variable was observed at $X = 1.06$. In Figure 1 we show the residuals between the standard and recovered magnitudes and colors for the observed Landolt standards. The total uncertainties of the zero points of our photometry are 0.02 mag for *BVI* magnitudes and 0.05 mag for the $U - B$ color. This estimate has been verified by a comparison with independently calibrated *BV* photometry for the same field collected during the 1998 season. The differences of the zero points between these two sets, calculated for 190 stars with $14 < V < 18$ amount to $\delta V = 0.000 \pm 0.015$ and $\delta(B - V) = 0.014 \pm 0.013$.

In Figure 2 we show *BVI* light curves of V209 phased with the ephemeris given in the following subsection. The variable exhibits only modest changes of $(B - V)$ and $(V - I)$ over the orbital cycle, with the colors becoming slightly redder during the primary eclipse, as is normally observed for distorted and gravity darkened components. The colors and

²IRAF is distributed by the National Optical Astronomy Observatories, which are operated by the Association of Universities for Research in Astronomy, Inc., under cooperative agreement with the NSF.

magnitudes of V209 at minima and at quadratures are listed in Table 2. In addition, we have measured $U - B = -0.023 \pm 0.009$ at phase 0.36. The primary eclipse is total with the phase of constant light lasting about $0.040P$. This can be seen in Figure 3 which shows a particularly well covered eclipse event. The small out-of-eclipse curvature of the light curve indicates that to first order proximity effects due to ellipsoidal shape of the components and the reflection effect are negligible. Therefore we adopt the magnitudes and colors observed at phase 0.0 as corresponding to the larger component of the system (with the convention that the primary component is the one with larger size and luminosity).

The light curve solution presented in Sec. 4 implies that the reflection effect in fact slightly modulates the light contributions of the individual binary components over the orbital period. Therefore, we did not attempt to measure the magnitudes and colors of the secondary component by subtracting the flux of the primary from the combined flux at maximum light.

2.2. Period Study

The observations collected with the du Pont telescope presented in this paper together with other data described in Kaluzny et al. (1996) as well as some unpublished observations collected with the 1-m Swope telescope at Las Campanas Observatory cover 9 individual primary eclipses. The times for these eclipses along with the timing errors determined using the method of Kwee & van Woerden (1956) are given in Table 3.

The O-C values listed in Table 3 correspond to the linear ephemeris:

$$MinI = HJD\ 2450963.67780(5) + 0.83441907(4) \quad (1)$$

determined from a least squares fit to the time-of-eclipse data. A linear ephemeris provides a good fit and there is no evidence for any detectable period change during the interval 1993–2003 covered by the data.

3. SPECTROSCOPIC OBSERVATIONS AND REDUCTIONS

Spectroscopic observations of V209 were obtained with the MIKE echelle spectrograph (Bernstein et al. 2003) on the Magellan II (Clay) telescope at Las Campanas Observatory. The data were collected during observing runs in March and June of 2004.

For this analysis we only use data obtained with the blue channel of MIKE, covering a range of 380 to 500 nm at a resolving power of $\lambda/\Delta\lambda \approx 38,000$. All of the observations were

obtained with a 0.7×5.0 arcsec slit and with 2×2 pixel binning. At 4380 \AA the resolution was ~ 2.7 pixels at a scale of 0.043 \AA/pixel . The seeing ranged from 0.7 to 1.3 arcsec. The spectra were first processed using a pipeline developed by Dan Kelson following the formalism of Kelson (2003, 2006) and then analyzed further using standard tasks in the IRAF/Echelle package. Each of the final spectra consisted of two 1200 s exposures interlaced with an exposure of a thorium-argon lamp. We obtained 11 spectra of V209. For the wavelength interval 400–500 nm, the average signal-to-noise ratio ranges from 25 to 45 depending on the observing conditions. In addition to observations of V209, we also obtained high S/N spectra of HD 4850 to be used as radial velocity templates.

3.1. Spectroscopic orbit of V209

In Figure 4 we show a section of a spectrum of V209 obtained near the orbital quadrature at phase 0.755 along with the spectrum of the template star. The only easily identifiable absorption feature besides the Balmer series lines is the Ca II K line located next to the interstellar line of the same ion; the narrow line inside He ϵ profile is due to the interstellar Ca II H line. The hydrogen lines are broad and the components from the individual component stars are strongly blended. We have analyzed the spectra of V209 using the broadening function (BF) formalism (Rucinski 2002). The BF analysis lets us study the effects of the spectral line broadening and binary revolution splitting even for relatively complicated profiles of the spectral lines. In the particular case of V209, the main advantage is through the use of intrinsically broad lines of hydrogen which are normally avoided in cross-correlation analyses.

A spectrum of HD 4850 ($V = 9.64$, $B - V = 0.03$, $Sp = A0V$ as given in SIMBAD)³ was used as a BF method template for V209. The color of HD 4850 closely matches the unreddened color of V209; we assumed a reddening of $E(B - V) = 0.131$ (Schlegel et al. 1998). According to Kinman et al. (2000) the other relevant properties of HD 4850 are as follows: $V_{rad} = -41.7 \text{ km/s}$, $V \sin i = 14 \text{ km/s}$, $[\text{Fe}/\text{H}] = -1.3$, $T_{eff} = 8450\text{K}$ and $\log(g) = 3.20$. We used the spectra in the wavelength range from 381 nm to 495 nm. Figure 5 presents examples of fitting a model to the BFs calculated for two spectra taken near opposite quadratures; the procedure used to model the BF is discussed in some detail in Kaluzny et al. (2006). The synchronized velocities of rotation, $V \sin i$ are 50 and 115 km s^{-1} for the primary and secondary components, respectively, and these values are confirmed by our BF modeling. Our velocity measurements for V209 are listed in Table 4 where we give the

³This research has made use of the SIMBAD database, operated at CDS, Strasbourg, France

heliocentric Julian date of mid-observation, the orbital phase, the measured radial velocity and the assigned weight for both components and then the primary and secondary ($O - C$) velocity deviations for the adopted orbit. The velocity observations and adopted orbit are presented in Figure 6. The current implementation of the BF method does not provide any internal estimates of errors of the measured radial velocities. The weights listed in Table 4 were assigned “a posteriori” based on the rms of the $O - C$ residuals for a given component and resulting from the fitted spectroscopic orbit. In practice we used an iterative approach starting from a spectroscopic solution with the assumed equal weights for both components. The velocity measured for the secondary components at phase 0.323 was assigned zero weight as it was derived from a relatively poorly defined peak in the BF.

A Keplerian orbit was fitted to the observations by fixing the period and epoch to the precise ephemeris given above. We assumed a circular orbit based on the photometric data. The adjustable parameters in the orbital solution were the velocity semi-amplitudes (K_1 and K_2) and the center of mass velocity V_0 . The fit was performed using the GAUSSFIT task within IRAF/STSDAS. The derived parameters of the spectroscopic orbit are listed in Table 5. The systemic velocity of the binary agrees with the radial velocity of ω Cen, $v_{rad} = 232.02$ km/s (van de Ven et al. 2006). At the location of V209 (about 7 arcmin from the cluster center) the velocity dispersion of ω Cen is about 11.5 km/s (van de Ven et al. (2006), Figure 3). We conclude that V209 is a radial velocity member of ω Cen.

4. LIGHT CURVE SOLUTION

We have analyzed the BVI light curves of V209 using the Wilson-Devinney model (Wilson & Devinney 1971) as implemented in the light-curve analyzing program MINGA (Plewa 1988). The mass-ratio of the binary was fixed at the spectroscopic value of $M_2/M_1 = 0.153 \pm 0.018$. The gravity darkening exponents and bolometric albedos were fixed at 1.0 and 1.0, respectively. The linear limb darkening coefficients were adopted from van Hamme (1993) for an assumed metallicity of $[\text{Fe}/\text{H}] = -1.7$ which corresponds to the mean metallicity of the cluster (Stanford et al. 2006). The effective temperature of the primary component was estimated from its color index, $B - V = 0.183 \pm 0.020$, measured at the phase of totality in the primary eclipse. The quoted uncertainty includes the external error arising from the photometric calibration. Schlegel et al. (1998) extinction maps imply a reddening of $E(B - V) = 0.131$, and using this value we obtain an unreddened color index for the primary component of $(B - V)_0 = 0.052 \pm 0.020$. An estimate of effective temperature of $T_1 = 9370 \pm 300$ K for the primary resulted from the use of the semi-empirical calibration of VandenBerg & Clem (2003).

The following parameters were adjusted in the light curve solution: the orbital inclination i , the non-dimensional potentials Ω_1 and Ω_2 , the effective temperature of the secondary T_2 , and the relative luminosity of the primary $L_1(B; V; I)$. The light curve solution obtained with MINGA is listed in Table 5 and the residuals between the observed and synthetic light curves are shown in Figure 7. In Table 6 we give the “equal volume” mean radii of the components. The solution implies that the difference between “polar” and the “point” radii amounts to about 2% for both components, the two radii being the radius toward the stellar pole and toward the Lagrangian point L1 of the binary orbit. The system has a detached configuration with both components showing only a very modest ellipsoidal distortion.

5. ABSOLUTE PARAMETERS

The absolute parameters of V209 obtained from our spectroscopic and photometric analysis are given in Table 7. The errors in the temperatures include all sources of uncertainties. The absolute visual magnitudes M_V were calculated by adopting bolometric corrections $BC_{V1} = -0.22$ and $BC_{V2} = -0.52$ which were derived from relations presented by Vandenberg & Clem (2003). There are two uncertainties involved in this step. First, we assumed $[\text{Fe}/\text{H}] = -1.7$, representing the peak in the wide distribution of metallicities measured for the ω Cen stars (Stanford et al. 2006). Second, the adopted bolometric corrections are appropriate for atmospheres of “normal” main-sequence stars while the chemical composition of the components of V209 was almost certainly affected by the evolution of the binary through a common-envelope phase.

We estimate the observed visual magnitudes of the components of V209 from the light curve solutions at maximum light as $V_1 = 16.825 \pm 0.021$, $B_1 = 17.015 \pm 0.021$, and $V_2 = 18.317 \pm 0.022$, $B_2 = 18.382 \pm 0.029$, where the uncertainties include the errors of the photometric zero point. This leads to apparent distance moduli $(m - M)_1 = 13.49 \pm 0.14$ and $(m - M)_2 = 13.51 \pm 0.12$ for components 1 and 2, respectively assuming the reddening of $E(B - V) = 0.131$ and using the absolute magnitudes from Table 7. Keeping in mind all of the sources of uncertainty mentioned above, we conclude that the derived distances are in reasonable agreement with other estimates of the cluster distance. For example van de Ven et al. (2006), using dynamical data, recently measured $(m - M)_0 = 13.75 \pm 0.13$. Our estimate of the distance of V209 provides an additional evidence that the binary belongs to ω Cen. Figure 8 shows the location of the individual components of the binary on a color-magnitude diagram (CMD) of the cluster. The less massive and hotter component of V209 is located on the CMD in the area occupied by stars from the extreme horizontal branch of the cluster. Its more massive companion is located between the blue stragglers

region and the blue horizontal branch.

6. DISCUSSION AND SUMMARY

In order to discuss the evolutionary status of V209 we compare the location of its components in the $T_{eff} - \log(g)$ diagram to that of several sdB stars in close binary systems in Figure 9. Data for the sdB stars were taken from Maxted et al. (2001) and Morales-Rueda et al. (2003). A sample of blue horizontal branch stars in globular clusters was taken from Behr (2003). The individual objects marked in Figure 9 include the visible component of the binary stars HD 188112 (Heber et al. 2003), the helium white dwarf SDSS J123410.37–022802.9 (Liebert et al. 2004), the visible component of the close binary M4–V46(NGC 6121–V46) (O’Toole et al. 2006) and the white dwarf SDSS J0917+46 (Kilic et al. 2006). These four objects have estimated masses spanning the range $0.17 - 0.24 M_{\odot}$. Also shown are evolutionary tracks for low-mass, post-red giant branch stars which lost their envelopes before core helium ignition (Driebe et al. 1998) as well as a location of zero-age (ZAHEB) and terminal-age (TAEHB) extreme horizontal branches (Dorman et al. 1993). The components of V209 have lower densities and effective temperatures compared with sdB stars in binaries. The secondary component of V209 has an effective temperature and a bolometric luminosity both too low for the star to be classified as a normal extreme horizontal branch star. Its mass is low, but it is within the range of masses observed for companions of white dwarfs in binaries (Nelemans & Tout 2005). Hence, it may be considered as a low mass star evolving toward the sdB or white dwarf stage.

Two recently identified low-mass helium white dwarfs have masses comparable to the secondary of V209. O’Toole et al. (2006) estimated a mass of $0.17 M_{\odot}$ for the field star SDSS J0917+46. Nothing is known for the moment about possible binarity of this object. A photometric variable V46 in the globular cluster M4 was shown by O’Toole et al. (2006) to be a single line spectroscopic binary whose visible component has a mass of about $0.19 M_{\odot}$. The orbital period of this system is about 2.1 hours and its invisible component is most likely a white dwarf with a lower mass limit of only $0.26 M_{\odot}$.

The mass of the primary component of V209 is too large to be a recently formed post-AGB star from ω Cen. The star is also more massive than most of helium white dwarfs from the field population. The mass distribution obtained for 1175 DA white dwarfs from the SDSS sample by Madej et al. (2004) shows a strong peak at $0.56 m_{\odot}$ and contains only about two dozen objects with masses exceeding $0.90 m_{\odot}$. The radius of the primary of V209 corresponds to that of a main sequence star of its mass. However, its luminosity as well as effective temperature are far too high to consider it a normal dwarf.

It is widely accepted that close binaries with degenerate components form through common-envelope (CE) evolution (Paczynski 1976). In particular, Han et al. (2003) studied some specific channels leading to the formation of binaries with sdB stars. We propose that V209 was formed through a process similar to the scenario called by these authors “the second common-envelope ejection channel”. It applies to systems consisting of a white dwarf (originally the more massive component of the binary) and a red giant. The binary evolved first through the CE phase when its primary ascended the giant branch. As a result of angular momentum loss the system became a close binary with an orbital period of the order of one day. At this stage it reached a detached configuration and consisted of a white dwarf and the main sequence companion. The second episode of the mass loss/transfer began once the companion entered the Hertzsprung gap. After losing most of its envelope it failed to ascend the red giant branch and to ignite helium in its core. Instead, it started to evolve along the horizontal direction on the H-R diagram moving toward the sdB domain. As for the primary component of the binary, it accreted an amount of mass sufficient for formation and ignition of a hydrogen shell on its surface. This led to an expansion of the photosphere and to the creation of a “re-born” star with an extended envelope. The former white dwarf is currently seen as the more massive and more luminous component of V 209 Cen while the less evolved component has lost most of its envelope and is currently composed of a helium core surrounded by a thin hydrogen shell. It is now seen as the less massive and hotter component of the binary. This kind of evolution was modeled in some detail by Burderi et al. (2002) and Ergma & Sarna (2003) who presented a scenario explaining the observed properties of the optical companion of the millisecond pulsar PSR J1740-5340.

An accurate explanation of an evolutionary status of V209 deserves further attention but it is beyond the scope of this paper to provide a detailed model for this peculiar binary. Admittedly, the above proposed evolutionary scenario is a highly speculative one. As it was pointed out by the referee, our scenario implies that the current primary would evolve very rapidly across the H-R diagram so that an *a priori* probability of seeing it at this short lasting phase of evolution is small. On the other hand, we note that ω Cen a is an exceptionally populous cluster with a rich population of hot subdwarfs. Also, we have failed to identify any other similar objects in the sample of 12 clusters surveyed for photometric variables during the CASE project. Hence, it is feasible that V209 has been caught – by a sheer luck – in this very short-lasting phase of its evolution.

In summary, V209 ω Cen, the second binary analyzed within the CASE project (after OGLEGC 17 = V212 ω Cen, Thompson et al. (2001); Kaluzny et al. (2002)), appears to be a very unusual star. In terms of its location on the color – magnitude diagram (Figure 8) and its very highly evolutionary modified properties, it is a very different binary from the main targets of the CASE project which are Main Sequence, detached binaries with unevolved and

moderately evolved components. Such binaries, which do not experience the preferential selection effects of V209, will be discussed in the subsequent publications of the CASE project.

We thank Dr. U. Heber for sending us the data defining location of model ZAEHB and TAEHB.

JK and WP were supported by the grants 1 P03D 001 28 and 76/E-60/SPB/MSN/P-03/DWM35/2005-2007 from the Ministry of Science and Information Society Technologies, Poland. IBT was supported by NSF grant AST-0507325. Support from the Natural Sciences and Engineering Council of Canada to SMR is acknowledged with gratitude.

REFERENCES

- Alard, C. 2000, *A&A*, 144, 363
- Alard, C., & Lupton, R.H. 1998, *ApJ*, 503, 325
- Behr, B.B. 2003, *ApJS*, 149, 67
- Bernstein, R., Shectman, S.A., Gunnels, S.M., Mochnecki, S., & Athey, A. E. 2003, *Instrument Design and Performance for Optical/Infrared Ground-based Telescopes*. Edited by Iye, Masanori; Moorwood, Alan F. M. *Proceedings of the SPIE*, 4841, 1694
- Burderi, L., D’Antona, F., & Burgcy, M. 2002, *ApJ*, 574, 325
- Clement, C. C. et al. 2001, *AJ*, 122, 2587
- Dorman, B., Rood, R.T., & O’Connell, R.W. 1993, *ApJ*, 466, 359
- Driebe, T., Schönberner, D., Blöcker, T., & Herwig, F. 1998, *A&A*, 339, 123
- Ergma, E., & Sarna, M. 2003, *A&A*, 399, 237
- Han, Z., Podsiadlowski, Ph., Maxted, P.F.L., & Marsh, T.R. 2003, *MNRAS*, 341, 669
- Heber, U., Edelmann, H., Lisker, T., & Napiwotzki, R. 2003, *A&A*, 411, L477
- Kaluzny, J., Kubiak, M., Szymański, M., Udalski, A., Krzemiński, W., & Mateo M. 1996, *A&AS*, 120, 139

- Kaluzny, J., Thompson, I., Krzeminski, W., Olech, A., Pych, W., Mochejska, B. 2002, in ASP Conf. Ser. 265, ω Centauri: A Unique Window into Astrophysics, ed. F. van Leeuwen, J. Hughes, G. Piotto (San Francisco: ASP), 155
- Kaluzny, J., Olech, A., Thompson, I.B., Pych, W., Krzemiński, W., & Schwarzenberg-Czerny, A. 2004, A&A, 424, 1101
- Kaluzny, J., et al. 2005, in AIP Conf. Proc. 752, Stellar Astrophysics with the World's Largest Telescopes, Ed. J. Mikołajewska & A. Olech (Melville, New York), 70
- Kaluzny, J., Pych, W., Rucinski, S.M., & Thompson, I.B. 2006, Acta Astron., 56, 237
- Kelson D.D. 2003, PASP, 115, 688
- Kelson D.D. 2006, AJ, submitted
- Kilic, M., Prieto, C.A., Brown, W.R., & Koester, D 2006, astro-ph/0611498
- Kinman, T., Castelli, F., Cacciari, C., Bragaglia, A., Harmer, D., & Valdes, F. 2000, A&A, 364, 102
- Kwee, K. K., & van Woerden, H. 1956, Bull. Astron. Inst. Netherlands, 12, 327
- Landolt, A.U. 1992, AJ, 104, 340
- Liebert, J., Bergerson, P., Eisenstein, D., Harris, H.C., Kleinman, S.J., Nitta, A., & Krzesiński, J. 2004, ApJ, 606, L147
- Madej, J., Nalezyty, M., & Althaus, L.G. 2004 A&A, 419, L5
- Maxted, P.F.L., Heber, U., Marsh, T.R., & North, R.C. 2001, MNRAS, 326, 1391
- Mochejska, B.J., Stanek, K.Z., Sasselov, D.D., Szentgyorgyi, A.H. 2002, AJ, 123, 3460
- Moni-Bidin, C., Moehler, S., Piotto, G., Recio-Blanco, A., Momany, Y., Méndez, R. A. 2006, A&A, 451, 499
- Moreles-Rueda, L., Maxted, P.F.L., Marsh, T.R., North, R.C, & Heber, U. 2003, MNRAS, 338, 752
- Napiwotzki, R. et al. 2004, Ap&SS, 291, 321
- Nelemans, G., & Tout, C.A. 2005, MNRAS, 356, 753

- O’Toole, S.J., Napiwotzki, R., Heber, U., Dreschel, H., Frandsen, S., Grundhal, F., & Bruntt, H. 2006, *Baltic Astronomy*, 15, 61
- Paczynski, B. 1976, in Eggleton P.P., Mitton S., Whelan J., eds, *Structure and Evolution of Close Binaries*. Kluwer, Dordrecht, p. 75
- Plewa, T. 1988, *Acta Astron.*, 38, 415
- Rucinski, S.M. 2002, *AJ*, 124, 1746
- Schlegel, D.J., Finkbeiner, D.P, Davis, M. 1998, *ApJ*, 500, 525
- Stanford, L.M., Da Costa, G.S., Norris, J.E., & Cannon, R.D. 2006, *ApJ*, 647, 1075
- Stetson, P.B. 1987, *PASP*, 99, 191
- Stetson, P.B. 1990, *PASP*, 102, 932
- Thompson, I. B. et al. 2001, *AJ*, 121, 3089
- VandenBerg, D.A., & Clem, J.L. 2003, *AJ*, 126, 778
- van de Ven, G., van den Bosch, R.C.E., Verolme, E.K., de Zeeuw, P.T. 2006, *A&A*, 445, 513
- van Hamme, W. 1993, *AJ*, 106, 2096
- Wilson, R.E., & Devinney, E.J. 1971, *ApJ*, 166, 605

Table 1. Summary of Photometric Observations of V209

Band	N	Exp Time sec	FWHM arcsec	<FWHM> arcsec
U	6	100-180	1.09-1.22	1.14
B	140	40-120	0.79-1.71	1.11
V	760	20-100	0.66-1.76	1.09
I	355	17-70	0.67-1.39	0.98

Table 2. *BVI* Photometry of V209 at Minima and Quadrature

Phase	<i>V</i>	<i>B</i>	<i>I</i>	<i>B</i> – <i>V</i>	<i>V</i> – <i>I</i>
Max	16.580	16.744	16.380	0.164	0.200
Min I	16.846	17.029	16.632	0.183	0.214
Min II	16.779	16.943	16.578	0.164	0.201

Table 3. Times of Minima and *O* – *C* Values for V209

Cycle	T_0 HJD-2400000	Error	<i>O</i> – <i>C</i>
-2255.5	49081.6456	0.0003	0.0000
-434.0	50601.5404	0.0002	-0.0005
0.0	50963.6777	0.0001	0.0001
3.5	50966.5983	0.0001	0.0000
6.0	50968.6842	0.0001	0.0001
2156.0	52762.6859	0.0005	-0.0006
2158.5	52764.7713	0.0002	0.0001
2159.5	52765.6057	0.0002	0.0001
2163.0	52768.5263	0.0001	0.0000

Table 4. Radial Velocities of V209 and Residuals from the Adopted Spectroscopic Orbit

HJD-2450000	phase	RV ₁	w ₁	RV ₂	w ₂	(O – C) ₁	(O – C) ₂
3182.5224	0.149	255.51	0.85	69.43	1.0	-3.62	-3.04
3182.5528	0.185	256.66	0.85	54.37	1.0	-5.92	4.51
3182.5829	0.221	263.42	0.85	26.31	1.0	-1.17	-10.34
3178.4959	0.323	270.18	0.85	99.67	0.0	8.25	45.56
3066.7032	0.347	268.31	0.85	65.56	1.0	8.73	-3.93
3178.5260	0.360	251.13	0.85	77.55	1.0	-6.76	-1.92
3066.7334	0.383	268.33	0.85	104.60	1.0	13.33	5.05
3179.6203	0.671	209.70	0.85	412.33	1.0	2.24	1.06
3068.7084	0.750	208.40	0.85	437.29	1.0	4.64	1.75
3180.5251	0.755	200.47	0.85	421.91	1.0	-3.31	-13.53
3068.7386	0.786	210.14	0.85	431.76	1.0	5.60	1.18

Table 5. Orbital Parameters for V209

Parameter	Value
P (days)	0.83441907(fixed)
T_0 (HJD-245 0000)	963.67780(fixed)
V_0 ($km\ s^{-1}$)	234.43 ± 1.49
e	0.0(fixed)
K_1 ($km\ s^{-1}$)	30.67 ± 2.39
K_2 ($km\ s^{-1}$)	201.11 ± 2.31
Derived quantities:	
$A \sin i$ (R_\odot)	3.824 ± 0.055
$M_1 \sin^3 i$ (M_\odot)	0.934 ± 0.040
$M_2 \sin^3 i$ (M_\odot)	0.142 ± 0.006

Table 6. Light Curve Solution for V209

Parameter	Value
i (deg)	85.03 ± 0.21
Ω_1	4.091 ± 0.025
Ω_2	2.815 ± 0.017
T_1 (K)	9370 (fixed)
$q = M_2/M_1$	0.153 (fixed)
T_2 (K)	10866 ± 122
(L_{1B}/L_{2B})	3.52 ± 0.09
(L_{1V}/L_{2V})	3.95 ± 0.10
(L_{1I}/L_{2I})	4.03 ± 0.19
$\langle r_1 \rangle$	0.2560 ± 0.0016
$\langle r_2 \rangle$	0.1106 ± 0.0013
rms (B) (mag)	0.0059
rms (V) (mag)	0.0075
rms (I) (mag)	0.0074

Table 7. Absolute Parameters for V209

Parameter	Value
A (R_\odot)	3.838 ± 0.055
M_1 (M_\odot)	0.945 ± 0.043
M_2 (M_\odot)	0.144 ± 0.008
R_1 (R_\odot)	0.983 ± 0.015
R_2 (R_\odot)	0.425 ± 0.008
T_1 (K)	9370 ± 300
T_2 (K)	10866 ± 323
L_1^{bol} (L_\odot)	6.68 ± 0.88
L_2^{bol} (L_\odot)	2.26 ± 0.28
M_{V1} (mag)	2.90 ± 0.13
M_{V2} (mag)	4.37 ± 0.12
$\log g_1$ (cm s^{-2})	4.43 ± 0.02
$\log g_2$ (cm s^{-2})	4.34 ± 0.02

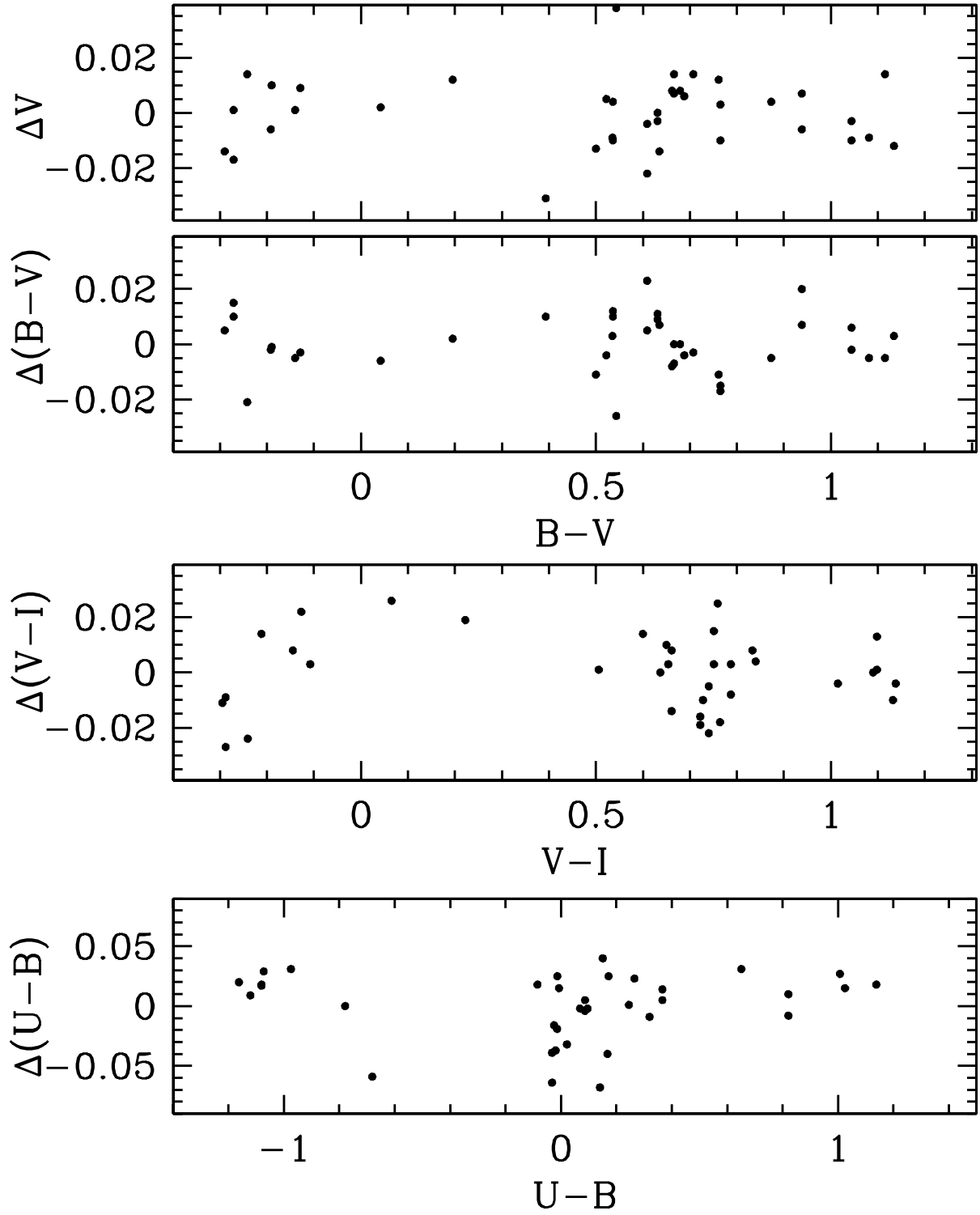


Fig. 1.— A plot of the color and magnitude residuals for the Landolt standard stars observed on the night of 2003 May 4.

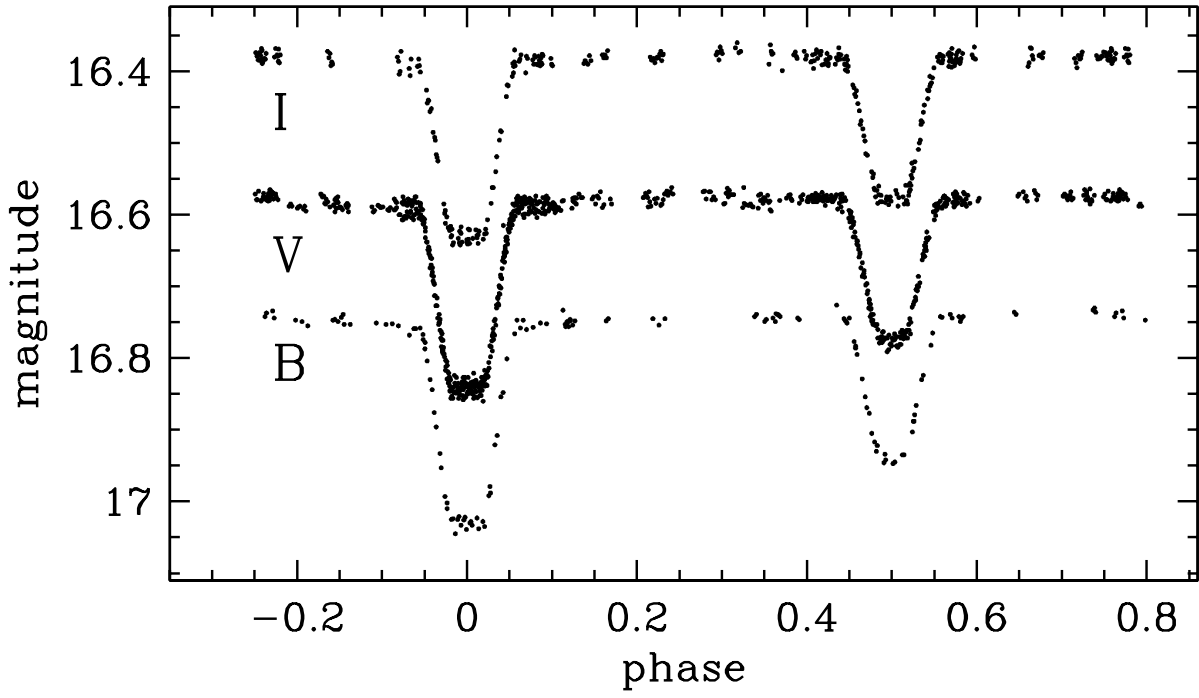


Fig. 2.— Phased *BVI* light curves of V209.

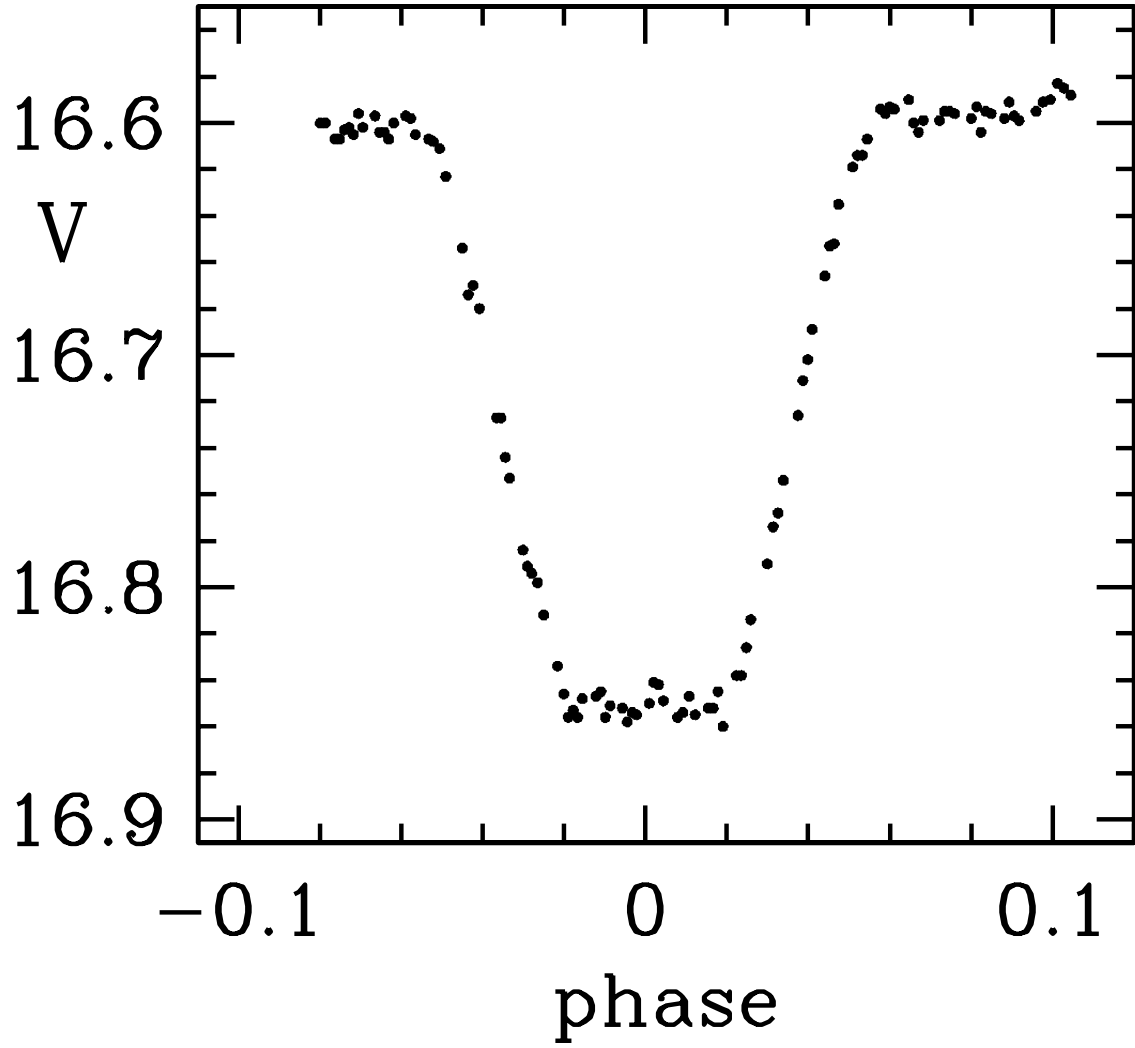


Fig. 3.— The V-band light curve of V209 in the primary eclipse.

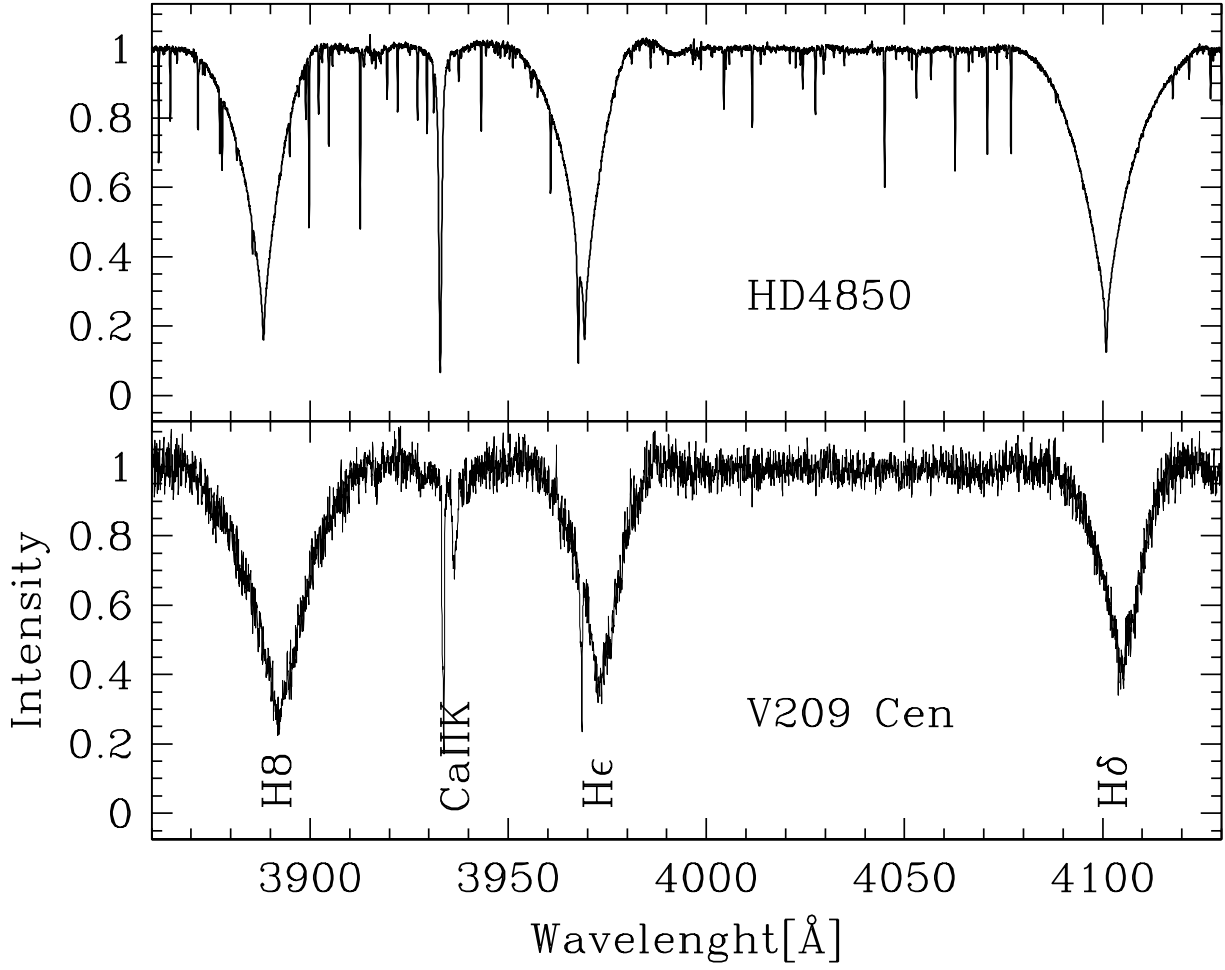


Fig. 4.— A sample spectrum of V209 taken at phase 0.755 (bottom) along with a spectrum of the template star (top).

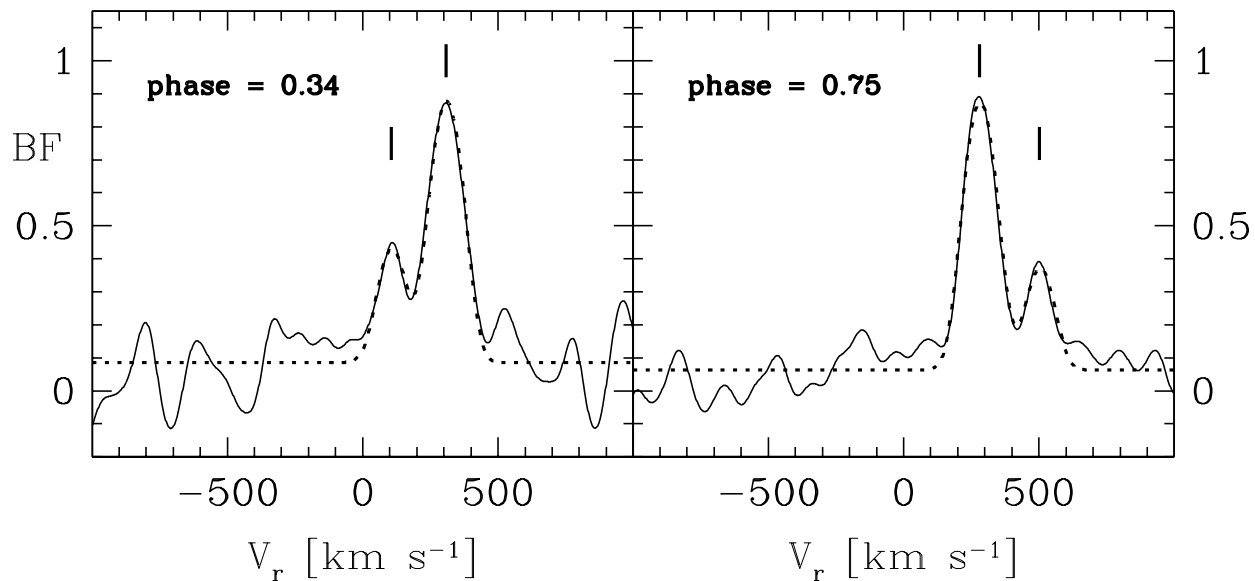


Fig. 5.— Broadening functions extracted from the spectra of V209 for obtained at orbital phases of 0.34 (left panel) and 0.75 (right panel). The dashed line shows the fit of a model BF to the observed one. The vertical ticks mark derived values of radial velocities.

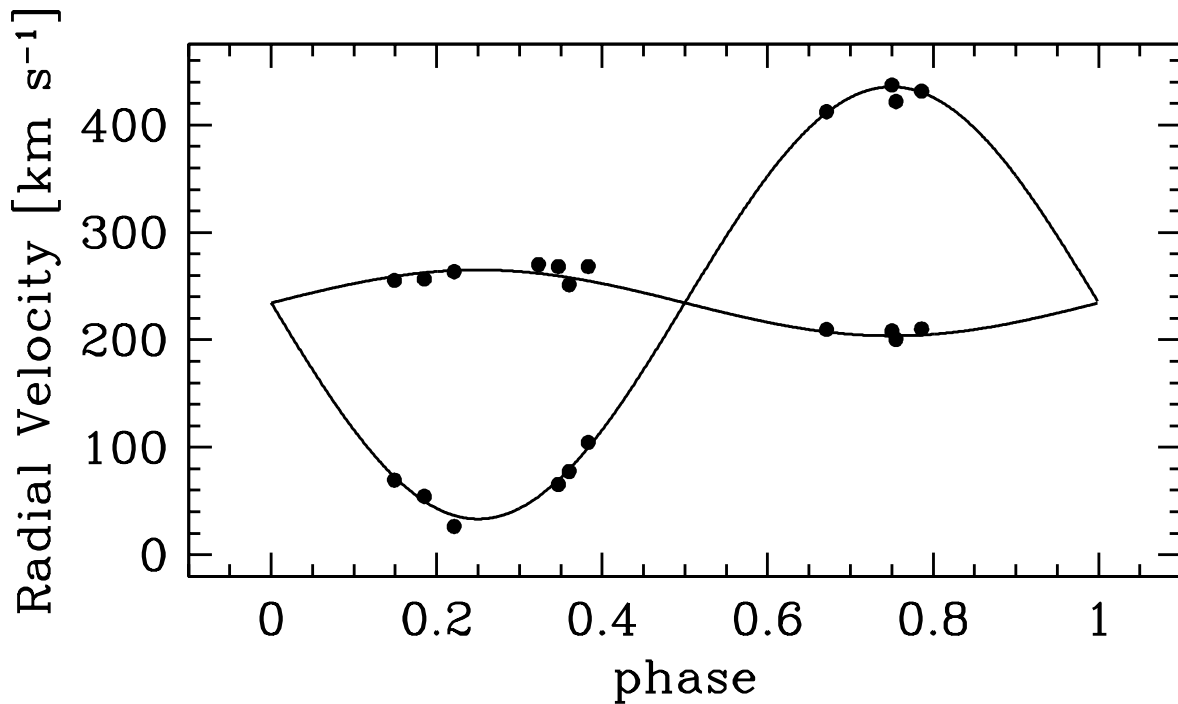


Fig. 6.— The spectroscopic observations and the adopted orbit for V209.

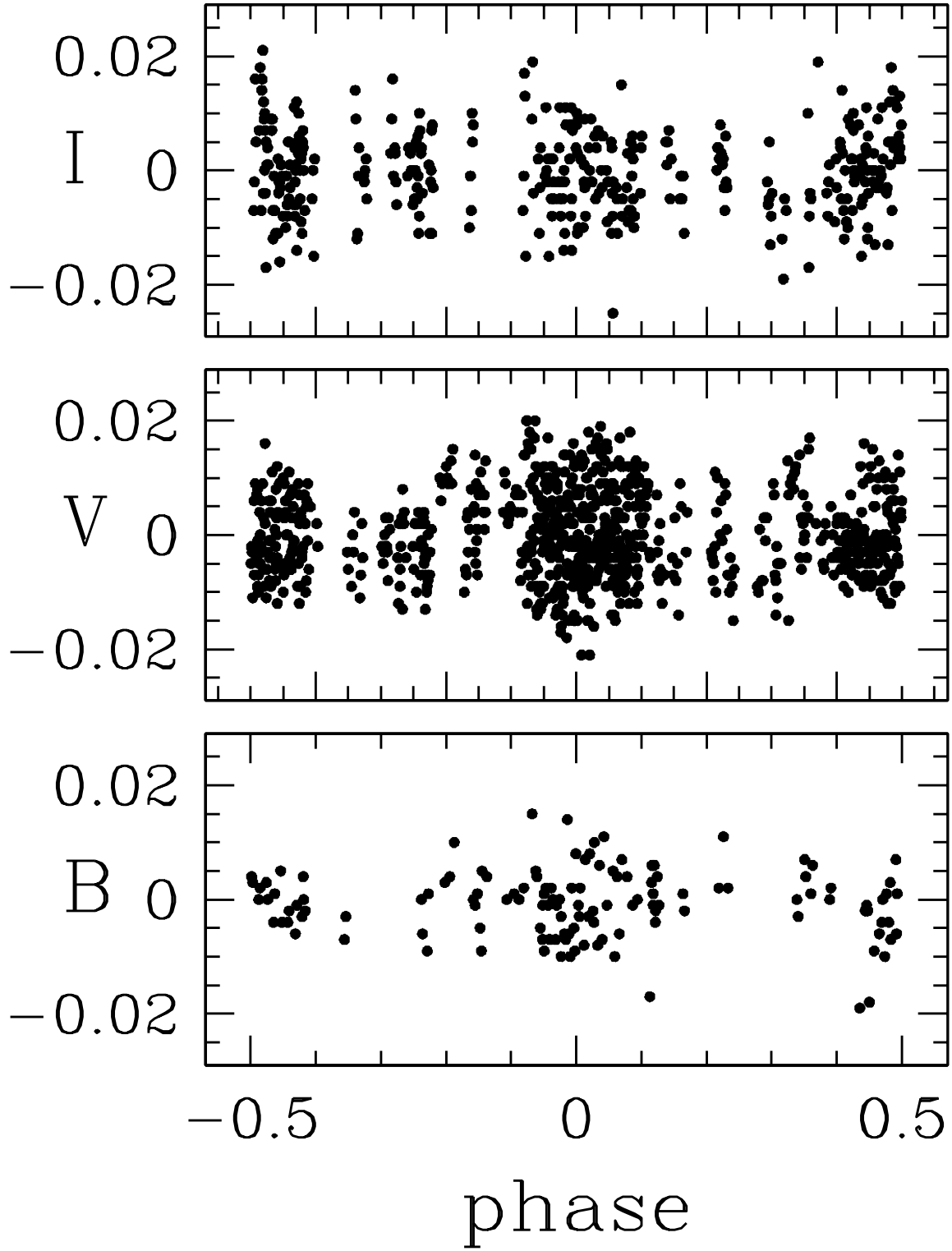


Fig. 7.— The residuals for the fit corresponding to the light curve solution.

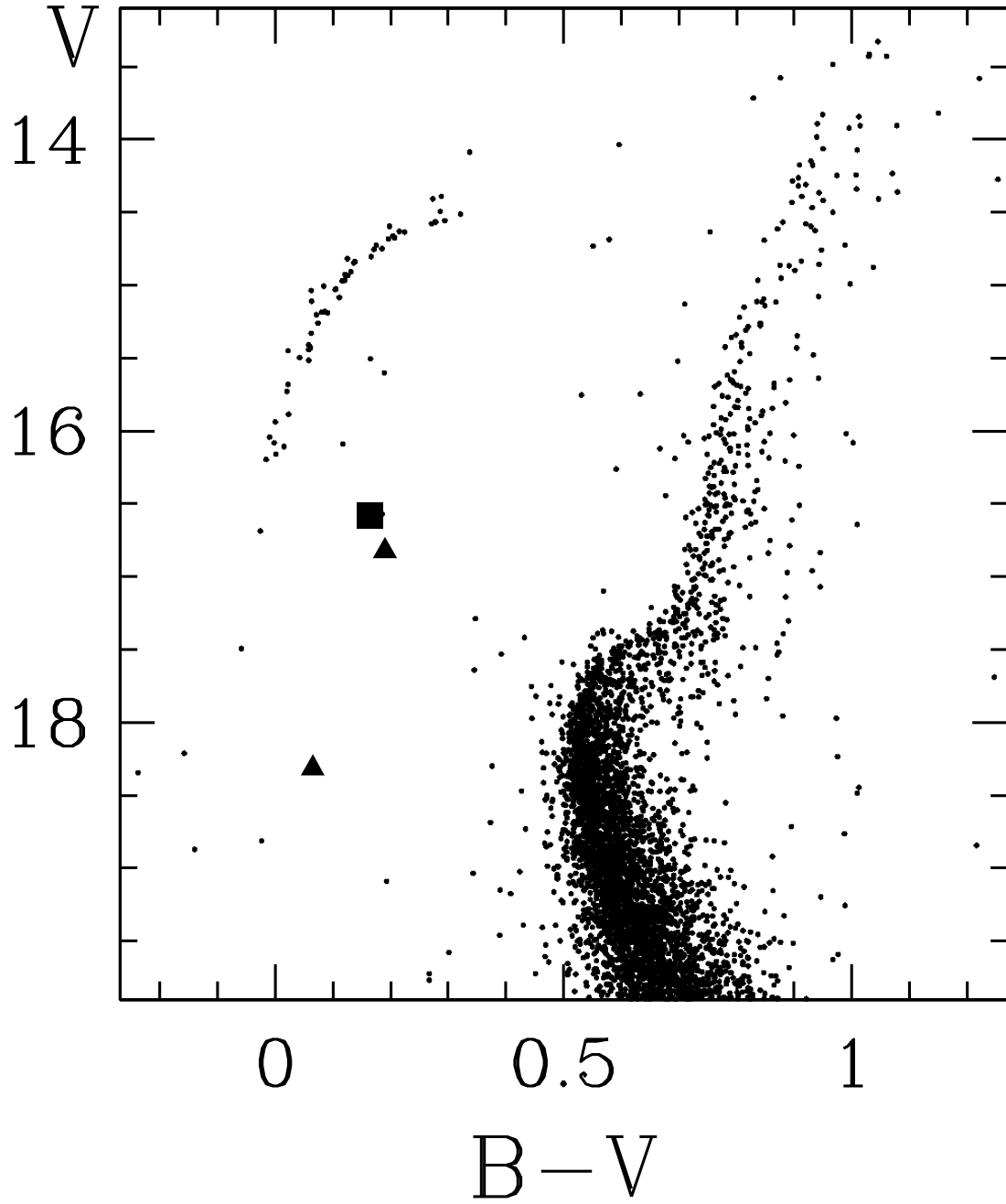


Fig. 8.— The color magnitude diagram for ω Cen stars near V209. The locations of both components of the binary are marked (filled triangles) along with the position of the combined photometric data (filled square).

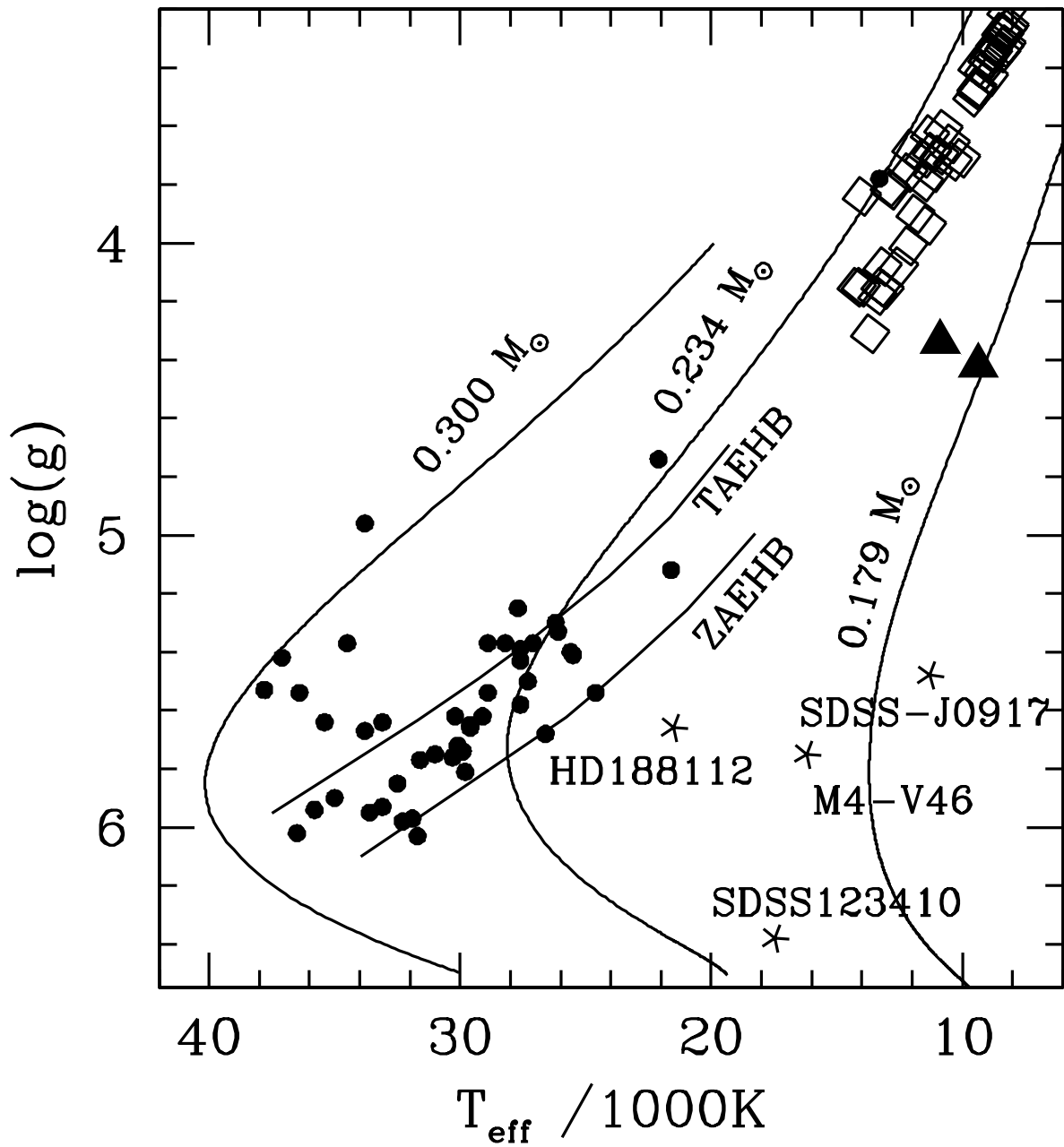


Fig. 9.— The position of the components of V209 (triangles) in the $(T_{\text{eff}}, \log g)$ plane. The locations of some sdB stars in close binaries are marked with dots while the open squares correspond to blue horizontal branch stars. The continuous lines labeled with stellar mass show evolutionary tracks for low-mass post-red giant-branch stars. See the text for more details.